Vectorial two-beam coupling with arbitrary shifted photorefractive gratings: An analytical approach

A. V. Khomenko and I. Rocha-Mendoza
Optics Department, CICESE, Carretera Tijuana-Ensenada km 107, A. P. 2732, Ensenada, B.C., Mexico
(Received 9 March 2004; revised manuscript received 23 August 2004; published 16 December 2004)

An analytical solution is presented to the vectorial coupled wave equations for the steady state amplitudes of two waves interacting in cubic photorefractive crystals. The solution accounts for pump depletion as well as an arbitrary phase shift between the interference pattern and photorefractive grating. It is shown that bidirectional vectorial amplification and polarization orthogonalization of the interacting beams take place in photorefractive crystal with diffusion, drift or mixed mechanism of space-charge formation.

DOI: 10.1103/PhysRevE.70.066615 PACS number(s): 42.70.Nq, 42.65.Hw

I. INTRODUCTION

The photorefractive two-wave mixing (TWM) allows an amplification of complex optical waves with high gain and high signal-to-noise ratio, which is a basis for many applications of photorefractive materials [1–3]. The requirements for the crystal sensitivity and response time vary strongly from one application to another, nevertheless the cubic photorefractive crystals nowadays meet the requirements of the biggest part of the potential applications. As a result, the cubic crystals of sillenite family (BSO, BTO, and BGO) and cubic semiconductors (InP, GaAs, and CdTe) have been the objects of many studies during the past years. All these crystals possess sufficiently strong response only when an external electric field, direct or alternating, is applied to assist in the photorefractive grating recording. The ac field enhances nonlocal photorefractive gratings, which are 90° phase shifted with respect to the interference pattern. The recording of local gratings with 0 or 180° shift is assisted by dc electric field. The nonlocal character of the photorefractive grating was considered for many years as the necessary condition for light amplification in nonlinear media [1–4]. Recently, the vectorial light amplification with unshifted local gratings in cubic photorefractive crystals was demonstrated [5]. This prompted us to develop a theory of the vectorial TWM, which include both local and nonlocal gratings as well as the case of an arbitrary phase shift between the interference pattern and the grating. The latter is important since in the majority of the experiments the phase shift does not equal strictly to 0 or 90°. Among the typical causes for this we can mention an almost unavoidable bias voltage in the experiments with ac field and the contribution of the diffusion mechanism of the space-charge formation in the experiments with dc field.

Recently, many experimental works were done with the samples of cubic crystals of high optical quality, long length of beam interaction and strong enhancement of the photorefractive response by high electric field [6–11]. These samples have allowed reaching high gain of signal waves when the depletion of the pump beam is inevitable. Therefore, it is of utmost importance for the realistic modeling of the vectorial TWM to include the effects of pump depletion, which were neglected in many previous works [12–16].

Our analysis is based on the vectorial equations for the steady-state amplitudes of the coupled waves in photorefractive crystal, the same as have been used in the other published works [5,10,16,17]. Many effects associated with the wave's polarization evolution caused by the vectorial TWM have been analyzed and understood using analytical or numerical solutions of these equations. In particular we have presented the numerical analysis of bidirectional light amplification in cubic crystals with local photorefractive gratings [5]. The numerical analysis should give a deep inside into mechanism of nonlinear optical effects due to inherent flexibility to explore and manipulate the model. Nevertheless analytical methods remain a powerful tool for the theoretical investigation of these phenomena and we apply it here to analyze in detail the vectorial bidirectional amplification in crystals with local, nonlocal and arbitrary shifted photorefractive gratings.

The organization of our paper is as follows: In Sec. II we describe a derivation of the coupled wave equations for the case of arbitrary phase shift between the photorefractive grating and interference pattern. We specify the crystal configurations, which should be analyzed using the results of present work, and restrictions of the model. In Sec. III we obtain the general solution of the coupled wave equations. Sections IV and V are devoted to the applications of the obtained solution to an analysis of the vectorial TWM in cubic crystals with local and nonlocal gratings. Finally, in Sec. VI we describe the peculiarities of TWM with gratings, which have the phase shift different from 0 and 90°.

II. THEORETICAL MODEL

We consider vectorial TWM in cubic photorefractive crystals without optical activity. Among these crystals are numerous photorefractive semiconductors of point group $\bar{4}3m$ (e.g., CdTe, GaAs, InP). The results obtained neglecting optical activity should be also applied in some extent to crystals of the sillenite family ($Bi_{12}SiO_{20}$ and $Bi_{12}TiO_{20}$), when the photorefractive response is strong enough. In this case the inter-beam coupling dominates and the coupling between the linearly polarized modes of each wave provoked by the optical activity can be neglected. Assuming a typical experimental configuration with the wave vector of the photore-

fractive grating parallel to the external electric field we exclude from consideration the refractive index changes induced by the external electric field. The birefringence induced by the external field affects the photorefractive TWM only in the crystals with optical activity and/or in the case of nonconcurrency between the external and space-charge fields. We write the coupled wave equations for steady-state amplitude vectors **S** and **R** of reference and signal waves using an approach similar to those of Refs. [11,16,17],

$$\frac{d\mathbf{S}}{dz} = \frac{ik_0 n^3 E_{SC}}{2}\hat{r}\mathbf{R},$$

$$\frac{d\mathbf{R}}{dz} = \frac{ik_0 n^3 E_{SC}^*}{2}\hat{r}\mathbf{S}, \tag{1}$$

where $k_0 = 2\pi/\lambda$ is the wave number, λ is the wavelength, n is the refractive index of the crystal, and E_{SC} is the complex amplitude of the space-charge field. The matrix $\hat{r}$ includes the effective electro-optic coefficients, which depend on the crystal cut. In the principal coordinate system this matrix has a diagonal form

$$\hat{r} = \begin{bmatrix} r_x & 0 \\ 0 & r_y \end{bmatrix}. \tag{2}$$

We calculate the complex amplitude of the space-charge field as

$$E_{SC} = E_{\max} m \exp(i\phi), \tag{3}$$

where $m = [S_x(z)R_x^*(z) + S_y(z)R_y^*(z)]/I_0$ is the depth of the interference pattern modulation, $S_x(z)$, $S_y(z)$, $R_x(z)$, and $R_y(z)$ are the linearly polarized components of the vector amplitudes **S** and **R** along the principal axes x and y, respectively, $I_0 = |S_x|^2 + |S_y|^2 + |R_x|^2 + |R_y|^2$ is the total light intensity, $E_{\max}$ is the maximum amplitude of the space-charge field, which should be reached, when $m = 1$. Equation (3) determines the linear dependence of the amplitude E_{SC} on the modulation depth of the interference pattern m, though in general this dependence should be in some extent nonlinear especially at high modulation depth [18,19]. In the present work, we do not consider the effects associated with the nonlinearity of the photorefractive response. Recently it was shown that the problem of nonlinear vectorial photorefractive TWM could be reduced to the linear one by a renormalization of the propagation coordinate [20]. The phase shift ϕ in Eq. (3) represents the spatial displacement of the space-charge field E_{SC} with respect to the interference pattern or, in other words, the phase shift between the photorefractive grating and the interference pattern.

An analytical solution of Eq. (1) can be found for the crystal configuration, which yields $r_x = -r_y$. This relation should be met with the crystal configurations shown in Fig. 1. In the first configuration [Fig. 1(a)], the direction of the light propagation coincides with the crystal axis [110], and the external field is applied along $[\bar{1}10]$. The principal x axis is directed at 45° angle counted from the $[\bar{1}10]$ direction, and the effective electro-optic coefficients are $r_x = -r_y = r_{41}$ without an elasto-optic contribution, where r_{41} is the component of the electro-optic tensor of a cubic crystal. In the second

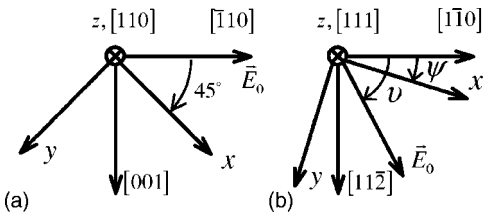

FIG. 1. Mutual orientations of crystal axes, the principal axes of the index ellipsoid x and y, and external electric field $\vec{E}_0$ for two configurations of cubic crystal. Light propagates along the z axis.

configuration [Fig. 1(b)], the light is directed along the crystal axis [111], while the external field should be applied in any transverse direction [1]. The principal x axis is directed at the angle $\psi = \pi/4 - \upsilon/2$, where υ is the angle between the direction of the external field E_0 and the [110] axis [1]. In this case the effective electro-optic coefficients are $r_x = -r_y = \sqrt{2/3}r_{41}$.

After the substitution of Eqs. (2) and (3) we rewrite Eq. (1) in the form

$$\frac{dS_x}{dz} = \frac{\Gamma}{2I_0}(S_x R_x^* + S_y R_y^*)R_x,$$

$$\frac{dS_y}{dz} = -\frac{\Gamma}{2I_0}(S_x R_x^* + S_y R_y^*)R_y,$$

$$\frac{dR_x}{dz} = -\frac{\Gamma^*}{2I_0}(S_x^* R_x + S_y^* R_y)S_x,$$

$$\frac{dR_y}{dz} = \frac{\Gamma^*}{2I_0}(S_x^* R_x + S_y^* R_y)S_y, \tag{4}$$

where $\Gamma = ik_0 n^3 r_x E_{\max}\exp(i\phi)$ is the complex coupling constant for the photorefractive grating, which has the ϕ shift with respect to the interference pattern.

The formally similar set of equations had been used previously for analysis of other nonlinear optical phenomena concerned with photorefractive wave coupling in cubic photorefractive crystals. Analytical solutions had been found for four-wave mixing and phase conjugation [21]. Later the similar theoretical approach was applied to the coupling mutually incoherent pairs of beams, which share a common grating [22]. The description of the polarization evolution were presented for vectorial unidirectional TWM [23,24]. In the present paper we focus our attention on the case of bidirectional vectorial TWM in cubic crystal with photorefractive gratings possessing complex coupling constants. In our case Eqs. (4) describe the coupling between x and y polarization modes of the two beams. The interference of x modes affects the coupling of y modes and vice versa via the intensity modulation responsible for the recording of the photorefractive grating. According to Eqs. (4) the amplitudes increments of x and y components have different signs. Taking into account the tensor nature of the photorefractive effect we should interpret this as a π-shift between the two refractive index gratings. One of them is responsible for the coupling between x-polarized components of two beams,

whereas the other couples *y*-polarized components. The energy flux associated with each polarization component has opposite direction in respect to each other that yields a bidirectional overall energy transfer between the beams as it will be shown below.

III. ANALYTICAL SOLUTION

Following to Refs. [2,21] we rewrite Eqs. (4) for new variables $u=S_x/R_y^*$ and $v=S_y/R_x^*$ as

$$\frac{du}{dz}=-\frac{\Gamma}{2I_0}(b^*u^2-\sigma u-b),$$

$$\frac{dv}{dz}=\frac{\Gamma}{2I_0}(b^*v^2+\sigma v-b), \tag{5}$$

where $\sigma=I_{0x}-I_{0y}$, $I_{0x}=|S_x|^2+|R_x|^2$, $I_{0y}=|S_y|^2+|R_y|^2$, and $b=S_xR_y+S_yR_x$. As a result of energy conservation and the reciprocity theorem I_{0x}, I_{0y}, and b are the constants of integration determined by the boundary conditions. The integration of Eqs. (5) gives

$$u=-\frac{s}{2b^*}\tanh\left[-\chi z+\tanh^{-1}\left(\frac{\sigma-2b^*u_0}{s}\right)\right]+\frac{\sigma}{2b^*},$$

$$v=-\frac{s}{2b^*}\tanh\left[\chi z-\tanh^{-1}\left(\frac{\sigma+2b^*v_0}{s}\right)\right]-\frac{\sigma}{2b^*}, \tag{6}$$

where $u_0=S_x(0)/R_y^*(0)$ and $v_0=S_y(0)/R_x^*(0)$ are the boundary conditions, $s=\sqrt{\sigma^2+4|b|^2}$ and $\chi=s\Gamma/4I_0$. Using the definitions and the constants of integration, the intensities of the polarization components can be written

$$I_{Rx}=\frac{I_{0x}-I_{0y}|u|^2}{1-|uv|^2},\quad I_{Ry}=\frac{I_{0y}-I_{0x}|v|^2}{1-|uv|^2},$$

$$I_{Sx}=|u|^2I_{Ry},\quad I_{Sy}=|v|^2I_{Rx}. \tag{7}$$

The solutions are valid for an arbitrary input polarization and arbitrary phase shift between the interference pattern and the refractive index grating, which allows analysis of the intensities evolution of the interacting beams as well as evolution of their polarizations.

IV. NONLOCAL GRATING, $\phi=90°$

First we analyze the analytical solution, Eqs (6), for the case of the nonlocal grating with $\phi=90°$, when the coupling constant Γ is a real number. To demonstrate how the direction of the energy flux depends on the polarization we rewrite the Eqs. (4) as increments of the beam intensities $I_S=I_{Sy}+I_{Sy}$ and $I_R=I_{Rx}+I_{Ry}$,

$$\frac{dI_S}{dz}=\frac{\Gamma}{I_0}(I_{Sx}I_{Rx}-I_{Sy}I_{Ry}),$$

$$\frac{dI_R}{dz}=-\frac{\Gamma}{I_0}(I_{Sx}I_{Rx}-I_{Sy}I_{Ry}). \tag{8}$$

The sign of the intensity increments and so the direction of energy flux depends on the sign of the factor $(I_{Sx}I_{Rx}-I_{Sy}I_{Ry})$. The **S**-beam increases its intensity, when the light polarization is along the *x* axis. The energy flux changes the direction for opposite if the beams have the orthogonal polarization. When the light is polarized along *x* or *y* axes, Eqs. (8) reduce to the well known case of scalar TWM, which was analyzed in many previous works. In the case of scalar TWM the energy flux in is unidirectional and coincides with the spatial shifts between the interference pattern and refractive index gratings, which are different for two orthogonal polarizations. The process of the beam interaction in a long crystal comes to the end when one of the beams is completely depleted so all its energy, which was not absorbed by the crystal, is transferred to the other beam.

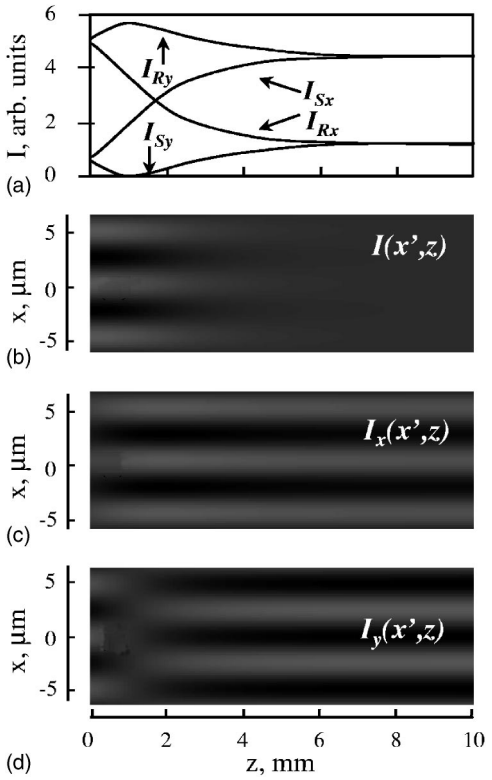

FIG. 2. Two beam coupling in a cubic crystal with local photorefractive grating. (a) Intensities of the polarization modes as functions of the propagation distance. Panels (b), (c), and (d) show the interference patterns $I(x',z)$, $I_x(x',z)$, and $I_y(x',z)$, respectively.

The solutions presented by Eqs. (6) and (8) yield the bidirectional amplification when both *x*- and *y*-polarization components are not zero at the input plane of the crystal. Figure 2 shows the calculation results for 45° input polarization, when $S_x(0)=S_y(0)$ and $R_x(0)=R_y(0)$. The calculations were done for the beam intensity input ratio 1:10 and the coupling constant $\Gamma=20$ cm^{-1}. To trace the phase changes of the polarization modes we present the fragment of the interference pattern calculated as the sum of the intensities of both polarization components, $I(x',z)=I_x(x',z)+I_y(x',z)$, where $I_i(x',z)=|S_i(z)|^2+|R_i(z)|^2+2|S_i(z)R_i(z)|\cos(Kx'+\varphi_i)$, $i=x,y$, K is the length of the grating vector, and φ_i is the phase difference between the complex amplitudes S_i and R_i. The axis x' coincides with the direction of the external field and the grating vector. Figure 2(a) shows that near input face

of the crystal, when $z<1$ mm, the intensity increments of different polarization components of the same beam have different signs, thus the total intensity of each beam is almost constant in this part of the crystal. The y-component of the weak beam, **S**, decreases and at the distance $z\approx 1$ mm it passes via the zero amplitude. At that point S_y changes the sign, so at $z>1$ mm $\varphi_y=180°$, while $\varphi_x=0$. The subsequent increment of the S_y-component leads to the decrement of the overall interference pattern contrast, as it is shown in Fig. 2(b). The energy exchange between the beams, as well as the changes of their polarization come to the end, when the modulation depth of the $I_y(x',z)$ interference pattern approaches the modulation depth of the $I_x(x',z)$ interference pattern that is $S_xR_x^*=-S_yR_y^*$. This relation means that the two beams have mutually orthogonal polarization and equal intensities. Recently the polarization orthogonalization of the beams interacting in cubic photorefractive crystals due to vectorial TWM or multiwave mixing has been predicted as a result of numerical study and demonstrated experimentally [25].

V. LOCAL GRATING, $\phi=0, 180°$

In the case of the local photorefractive response $\Gamma=i\beta$, where β is real and we rewrite Eqs. (4) as increments of the beam intensities and phase shifts in the form

$$\frac{dI_S}{d_Z}=-4\beta\frac{V}{I_0}\sin\varphi_{xy},$$

$$\frac{dI_R}{d_Z}=4\beta\frac{V}{I_0}\sin\varphi_{xy},$$

$$\frac{d\varphi_x}{d_Z}=-\frac{\beta}{I_0}(I_{Rx}-I_{Sx})-\beta\frac{V(I_{Rx}-I_{Sx})}{I_0I_{Rx}I_{Sx}}\cos\varphi_{xy},$$

$$\frac{d\varphi_y}{d_Z}=\frac{\beta}{I_0}(I_{Ry}-I_{Sy})+\beta\frac{V(I_{Ry}-I_{Sy})}{I_0I_{Ry}I_{Sy}}\cos\varphi_{xy}, \qquad (9)$$

where $V=\sqrt{I_{Sx}I_{Sy}I_{Rx}I_{Ry}}$ and φ_{xy} is the phase shift between the interference patterns of x and y polarization components, $\varphi_{xy}=\varphi_x-\varphi_y$.

Equations (9) are reduced to the case of the scalar TWM, when the interacting beams have only x or y polarization component, which gives $V=0$. In this case, the obtained expressions predict the well-known fact that in the photorefractive crystal with the local response the interacting beams do not change the intensities, nevertheless the phase changes yield the inclination of the fringes of the interference pattern. In the case of vectorial TWM, when the beams have both polarization components, so $V\neq 0$, the energy exchange between the beams is possible even in the crystal with the local photorefractive response. The second condition for the nonzero energy flux between the beams is a nonzero phase shift between the interference patterns of the two polarization component $I_x(x',z)$ and $I_y(x',z)$, i.e., $\varphi_{xy}\neq 0$. As an example, both conditions, $V\neq 0$ and $\varphi_{xy}\neq 0$, should be met when one beam has a 45° polarization, while the other beam has circular or elliptic polarization. If we consider the net effect of the beam interaction in the long photorefractive crystal, the condition $\varphi_{xy}\neq 0$ is not mandatory for the energy exchange between beams. Equations (9) show that the phase increments $d\varphi_x/dz$ and $d\varphi_x/dz$ have opposite signs. Thus, vectorial TWM first yields the phase shift between the interference patterns of the polarization components without energy exchange between beams. In turn, the nonzero phase shift results in the change of the beam intensities. The signs of the intensity increments and so the direction of the energy flux between the beams depends on the sign of the phase shift φ_{xy}. If the intensity of the **R** beam is higher than the intensity of the **S** beam, then $d\varphi_{xy}/dz<0$ results in the energy transfer from **R** to **S** beam. In the opposite case, when the **S** beam is stronger, Eqs. (9) give $d\varphi_{xy}/dz>0$ and the energy flux is in the opposite direction. Thus the vectorial beam coupling in the photorefractive crystal with local grating always yields the amplification of the weak beam independently of the mutual position of the strong and weak beam, in other words, the amplification is bidirectional.

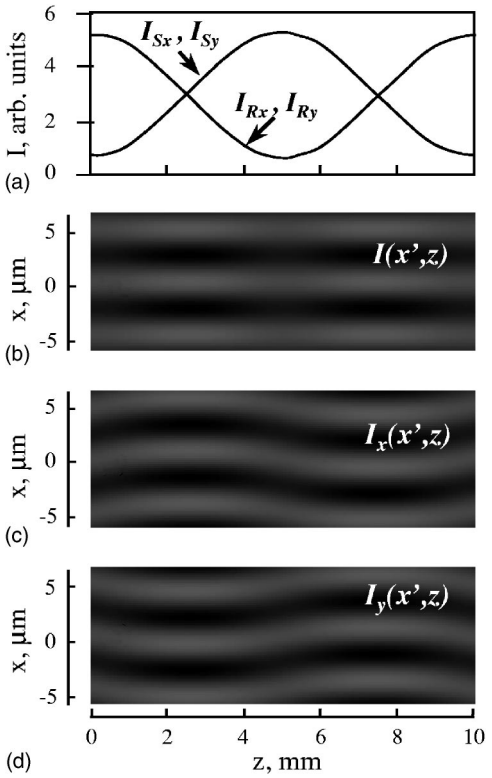

FIG. 3. The same as Fig. 2 but for the crystal with local photorefractive grating.

Figure 3 shows the vectorial beam coupling in the photorefractive crystal with local response. These results were calculated using Eqs. (9) for the beams with the intensity ratio 1:10, the coupling constant $\beta=20$ cm^{-1}, and the 45° polarization of the beams at the input of the crystal. In our previous work the similar results have been obtained as a numerical solution of the vectorial equations for steady-state TWM [5]. As one can see in Fig. 3, near the input face of the crystal ($z=0$) the fringes of the interference pattern $I_x(x',z)$ are bended in the opposite direction with respect to the fringes of

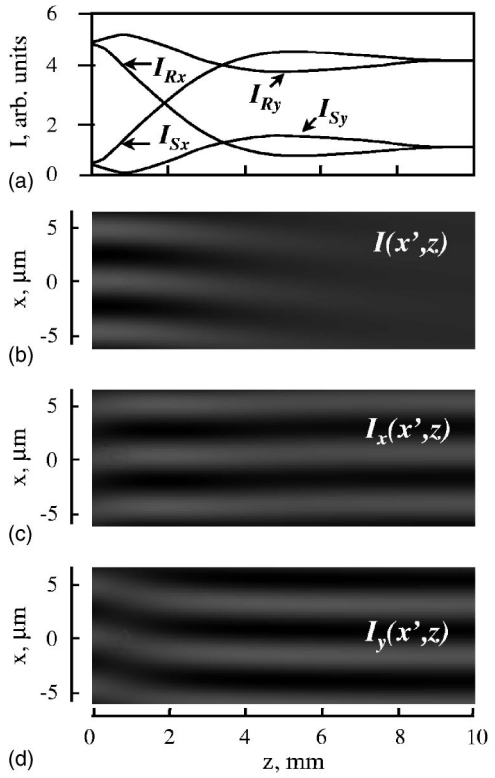

FIG. 4. The same as Fig. 2 but for the crystal with 45° shifted photorefractive grating.

$I_y(x',z)$, which results in nonzero phase shift φ_{xy}. The overall interference pattern, $I(x',z)=I_x(x',z)+I_y(x',z)$, has straight fringes with a constant contrast. In the long photorefractive crystal the phase shift φ_{xy} periodically changes the sign that results in periodical inversion of the energy transfer between two beams along the z axis.

VI. GRATINGS WITH ARBITRARY SHIFT ϕ

A. Vectorial TWM

As was shown above, the vectorial beam coupling in the crystal with unshifted photorefractive grating ($\phi=0$, 180°) yields the monotonic changes of the beam intensities and polarizations. If the crystal is long enough, the coupling results in equal intensities and orthogonal polarizations of the beams at the output of the crystal. On the other hand, in the crystal with nonlocal response, when $\phi=\pm 90°$, two beams periodically exchange by the intensities. Figure 4 shows the beam coupling in the intermediate case, when $\phi=45°$. The results were calculated using the similar parameters as before: the intensity input ratio 1:10, 45° polarization at input of the crystal, and the coupling constant $|\Gamma|=20\ \mathrm{cm}^{-1}$.

In the intermediate case of the grating, the vectorial beam coupling has similarities both with the local and nonlocal cases. The beam intensities oscillate along the direction of propagation due to the periodical inversion of the energy transfer between the beams as in the case of the local grating. At the same time the oscillations are damped and the intensities approach a steady state, which coincides with what we

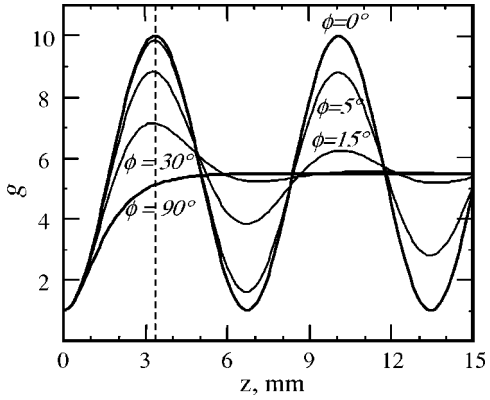

FIG. 5. Photorefractive gain as a function of the propagation distance plotted for different phase shifts ϕ between the interference pattern and photorefractive grating.

have discussed in the case of the nonlocal grating: the output intensities of the beams are equal and the polarizations are orthogonal. The fringes of the interference patterns are bended, which is the specific feature of the beam coupling with the local grating. At the same time Fig. 4 shows the decrease of the contrast of the overall interference pattern $I(x',z)$, similar to what has been shown for the nonlocal grating. These features of the beam coupling reveal in the dependence of the photorefractive gain on the propagation distance, which is shown in Fig. 5. The gain was calculated as a ratio $g(z)=[|S(z)|^2/|S(0)|^2]$ for the coupling constant $|\Gamma|=32.5\ \mathrm{cm}^{-1}$ and the input intensity ratio $\xi=[|R(0)|^2/|S(0)|^2]=10$. In the case of nonlocal grating, when $\phi=90°$, the gain monotonically approaches the saturation value $g_s=(\xi+1)/2$ with the increase of the propagation distance. When the gating is local, i.e., $\phi=0$, the gain oscillates around this value as

$$g(z)=[(\xi-1)\sin^2(\pi z/L_p)+1], \tag{10}$$

and the beam exchange by the intensities at the distance $L_p/2$, where $L_p=\lambda/n^3 r|E_{SC}|$ [5]. All curves calculated for the arbitrary phase shift ϕ situate between two extreme curves, which correspond to the local and nonlocal gratings. Note that for short interacting distances, $z<5$ mm, the local grating ($\phi=0$) yields the maximum amplification in comparison with the gratings with any other phase shift. Obviously, this result, which is valid for 45° input polarization, is not valid in general. The polarization dependence of the gain is presented in Fig. 6 for different grating phase shifts ϕ. The calculations were done using the same parameters as we used to obtain the results presented in Fig. 5 and the crystal length $z=3.25$ mm. This length approximately corresponds to the first maximum of the gain for the local grating (see Fig. 5). Comparing the results presented in Figs. 5 and 6 we came to the conclusion that absolute maximum of the photorefractive amplification should be reached with the nonlocal grating ($\phi=90°$) and the linear polarization aligned along one of the principal axes of the index ellipsoid. However, when the photorefractive response is local ($\phi=0$) the gain reaches maximum at 45° and −45° polarizations, when two polarization modes have equal input amplitudes. This prediction has

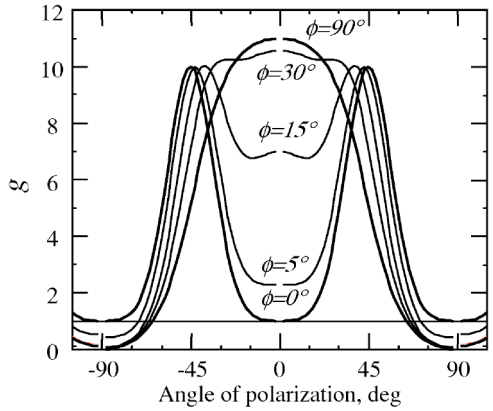

FIG. 6. Gain versus polarization angle for different phase shifts of the photorefractive grating.

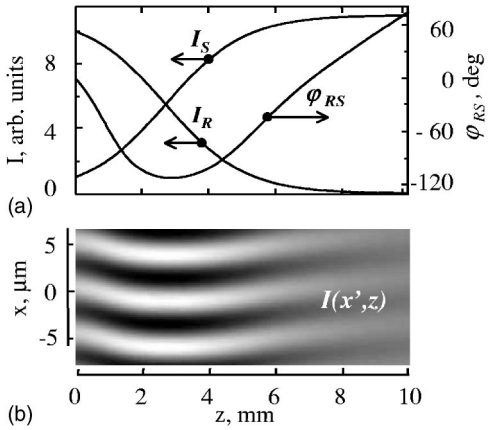

FIG. 7. Scalar TWM with the 45°-shifted photorefractive grating. (a) Wave intensities and relative phase shift as functions of the propagation distance. (b) Interference pattern of the interacting waves.

been confirmed experimentally in Ref. [5]. Similar to the results presented in Fig. 5, the polarization dependence of the gain for the arbitrary phase shift ϕ is somewhat in the middle between the case of the local and nonlocal gratings.

B. Scalar TWM

TWM turns into its scalar version when the input polarization of the two waves coincides with one of the two polarization modes. In other words, when the polarization angle α is equal to 0°or 90°. Owing to the definition, the variables u and v have a singularity at $\alpha=0°$ and 90°. Thus the scalar TWM cannot be described directly by Eqs. (6) and (7) and so the curves in Fig. 6 have breaks out at the angles, which are corresponding to the polarization eigenmodes. Nevertheless the polarization mode intensities presented by Eqs. (7) converge to finite limits as $\alpha\to 0°$ or $\alpha\to 90°$. These limits are the solution for the scalar TWM, which is given by

$$I_S = I_0 \frac{|u_0|^2\left(1-|v_0|^2\right)}{1-|u_0 v_0|^2}, \quad I_R = I_0 \frac{1-|u_0|^2}{1-|u_0 v_0|^2}, \tag{11}$$

where

$$u_0 = \lim_{\alpha\to 0} \alpha u = \frac{1}{\sqrt{\xi}} \frac{1+\tanh \chi z}{1-\dfrac{\xi-3}{\xi+1}\tanh \chi z},$$

$$v_0 = \lim_{\alpha\to 0} \frac{v}{\alpha} = \frac{1}{\sqrt{\xi}} \frac{1-\dfrac{3\xi-1}{\xi+1}\tanh \chi z}{1-\tanh \chi z}. \tag{12}$$

Here I_0 is the total intensity and ξ is the input intensity ratio. According to the definitions of u_0 and v_0, the relative phase of the two waves can be written as

$$\varphi_{RS} = -i \ln \frac{u_0}{v_0}\left|\frac{v_0}{u_0}\right|. \tag{13}$$

When $\chi=\chi^*$, the grating is nonlocal and the obtained solutions (11)–(13) reduces to the well-known relations for the wave intensities and relative phase [2,3]

$$I_S = \frac{I_0}{1+\xi \exp(-\chi z)}, \quad I_R = \frac{I_0}{1+\xi^{-1}\exp(\chi z)}, \quad \varphi_{RS} = 0. \tag{14}$$

Here the energy flux is unidirectional and the energy of one of the waves should be completely transferred to the other wave. In the case of local grating ($\chi=-\chi^*$) Eqs. (11)–(13) predict that wave intensities are constant, while the relative phase experiences a change always when two waves have different intensities, which is also a well-known result [2,3].

Obtained solutions (11)–(13) for the scalar TWM is useful for an analysis of scalar TWM with arbitrary shifted photorefractive grating. Figure 7 shows the result calculated using these relations for the grating with intermediate shift, $\phi=45°$. Here the changes of the wave intensities and the relative phase take place simultaneously. The sign of the increment of φ_{RS} depends on the wave intensity ratio. In our calculations $\chi>0$, which leads to the negative increment of φ_{RS} near the input of the photorefractive crystal, when $I_S<I_R$. TWM results in an increase of I_S, and the increment of φ_{RS} changes the sign as the S-wave intensity becomes bigger than I_R. The changes of the relative phase result in V-shaped fringes of the interference pattern of the interacting waves as it is shown in Fig. 7(b).

VII. CONCLUSIONS

We have presented an analytical solution of the coupled-wave equations for vector wave amplitudes that describe the degenerate two beam coupling in cubic crystal with arbitrary phase shift between the interference pattern and photorefractive grating. The developed theory allows the analytical description of the beam coupling when both interacting beams experience strong changes of intensities and polarizations, thus the approximation of a uniform grating is not acceptable. It has been shown that the theory describes such effects

as the bidirectional amplification of the weak beam, polarization orthogonalization and the bending of the interference pattern fringes in cubic photorefractive crystal. We have demonstrated the effect of the photorefractive gain oscillations and discussed the polarization dependence of the gain for arbitrary shifted gratings.

ACKNOWLEDGMENTS

Financial support from Consejo Nacional de Ciencia y Tecnología, Mexico (Project No. 44006) is greatly acknowledged. We thank M. A. García Zarate for valuable technical assistance.

[1] M. P. Petrov, S. I. Stepanov, and A. V. Khomenko, *Photorefractive Crystals in Coherent Systems* (Springer-Verlag, Berlin, 1991).
[2] P. Yeh, *Introduction to Photorefractive Nonlinear Optics* (Wiley, New York, 1993).
[3] L. Solymar, D. Webb, and A. Grunnet-Jepsen, *The Physics and Applications of Photorefractive Materials* (Clarendon, Oxford, 1996).
[4] R. W. Boyd, *Nonlinear Optics* (Academic, San Diego, 1992).
[5] I. Rocha-Mendoza and A. V. Khomenko, Opt. Lett. **27**, 1448 (2002).
[6] A. A. Kamshilin, R. Silvennoinen, T. Jaaskelainen, C. J. de Lima, M. R. B. Andreeta, and V. V. Prokofiev, Opt. Lett. **18**, 690 (1993).
[7] A. A. Kamshilin, T. Jaaskelainen, A. V. Khomenko, and A. Garcia-Weidner, Appl. Phys. Lett. **67**, 2585 (1995).
[8] A. V. Khomenko, A. Garcia-Weidner, and D. Tentori, Opt. Lett. **21**, 776 (1996).
[9] A. V. Khomenko, E. Nippolainen, A. A. Kamshilin, A. Zuniga Segundo, and T. Jaaskelainen, Opt. Commun. **150**, 175 (1998).
[10] E. Shamonina, K. H. Ringhofer, B. I. Sturman, V. P. Kamenov, G. Cedilnik, M. Esselbach, A. Kiessling, R. Kowarschik, A. A. Kamshilin, V. V. Prokofiev, and T. Jaaskelainen, Opt. Lett. **23**, 1435 (1998).
[11] C. A. Fuentes-Hernández and A. V. Khomenko, Phys. Rev. Lett. **83**, 1143 (1999).
[12] A. Marrakchi, R. V. Johnson, and A. R. Tanguay, J. Opt. Soc. Am. B **3**, 321 (1986).
[13] S. Mallick, D. Rouede, and A. G. Apostolidis, J. Opt. Soc. Am. B **4**, 1247 (1987).
[14] A. Brignon and K. H. Wagner, Opt. Commun. **101**, 239 (1993).
[15] B. I. Sturman, D. J. Webb, R. Kowarschik, E. Shamonina, and K. H. Ringhofer, J. Opt. Soc. Am. B **11**, 1813 (1994).
[16] B. I. Sturman, E. V. Podivilov, K. H. Ringhofer, E. Shamonina, V. P. Kamenov, E. Nippolainen, V. V. Prokofiev, and A. A. Kamshilin, Phys. Rev. E **60**, 3332 (1999).
[17] G. F. Calvo, B. I. Sturman, F. Agullo-Lopez, M. Carrascosa, A. A. Kamshilin, and K. Paivasaari, J. Opt. Soc. Am. B **19**, 1564 (2002).
[18] G. A. Brost, J. Opt. Soc. Am. B **9**, 1454 (1992).
[19] G. F. Calvo, B. I. Sturman, F. Agullo-Lopez, M. Carrascosa, A. A. Kamshilin, and K. Paivasaari, J. Opt. Soc. Am. B **19**, 1564 (2002).
[20] B. I. Sturman and O. S. Filippov, Phys. Rev. E **68**, 036613 (2003).
[21] M. Cronin-Golomb, J. O. White, B. Fischer, and A. Yariv, Opt. Lett. **7**, 313 (1982).
[22] R. Saxena, F. Vachss, and P. Yeh, J. Opt. Soc. Am. B **7**, 1210 (1990).
[23] B. Fischer, J. O. White, M. Cronin-Golomb, and A. Yariv, Opt. Lett. **11**, 239 (1986).
[24] P. Yeh, J. Opt. Soc. Am. B **9**, 1382 (1987).
[25] I. Rocha-Mendoza and A. V. Khomenko, J. Opt. Soc. Am. B **21**, 770 (2004).